

Low-temperature heat transport and magnetic-structure transition of the hexagonal TmMnO_3 single crystals

X. M. Wang,¹ Z. Y. Zhao,¹ C. Fan,¹ X. G. Liu,¹ Q. J. Li,¹ F. B. Zhang,¹ L. M. Chen,² X. Zhao,³ and X. F. Sun^{1,*}

¹*Hefei National Laboratory for Physical Sciences at Microscale,
University of Science and Technology of China, Hefei, Anhui 230026, People's Republic of China*

²*Department of Physics, University of Science and Technology of China,
Hefei, Anhui 230026, People's Republic of China*

³*School of Physical Sciences, University of Science and Technology of China,
Hefei, Anhui 230026, People's Republic of China*

(Dated: June 29, 2018)

We study the low-temperature heat transport, as well as the magnetization and the specific heat, of TmMnO_3 single crystals to probe the transitions of magnetic structure induced by magnetic field. It is found that the low- T thermal conductivity (κ) shows strong magnetic-field dependence and the overall behaviors can be understood in the scenario of magnetic scattering on phonons. In addition, a strong “dip”-like feature shows up in $\kappa(H)$ isotherms at 3.5–4 T for $H \parallel c$, which is related to a known spin re-orientation of Mn^{3+} moments. The absence of this phenomenon for $H \parallel a$ indicates that the magnetic-structure transition of TmMnO_3 cannot be driven by the in-plane field. In comparison, the magnetothermal conductivity of TmMnO_3 is much larger than that of YMnO_3 but smaller than that of HoMnO_3 , indicating that the magnetisms of rare-earth ions are playing the key role in the spin-phonon coupling of the hexagonal manganites.

PACS numbers: 66.70.-f, 75.47.-m, 75.50.-y, 75.85.+t

I. INTRODUCTION

The hexagonal manganites RMnO_3 ($R = \text{Y}, \text{Ho}, \text{Er}, \text{Tm}, \text{Yb}, \text{and Lu}$) have been extensively studied because of their multiferroicity.^{1–12} In these materials, the ferroelectric order is formed at temperatures as high as 800 K, which results from the ionic displacements breaking the inversion symmetry of the lattice. The Mn^{3+} moments develop the antiferromagnetic (AF) ordering below $T_{N,Mn} = 70\text{--}90$ K. The magnetoelectric coupling has been found to be strong between the c -axis polarization and the ab -plane staggered AF magnetization at low temperatures, as the strong dielectric anomalies at the magnetic phase transitions have demonstrated.^{6,10,13} Naturally, the magnetic structures and their transitions driven by changing temperature or magnetic field^{5,7} are the central issues of the magnetoelectric coupling in these compounds, which are still not fully understood due to the complexity of Mn^{3+} and R^{3+} magnetism.

The Mn^{3+} ions form triangular planar sublattices and the AF exchange coupling among Mn^{3+} moments is therefore geometrically frustrated. As a result, below $T_{N,Mn}$, the Mn^{3+} moments are ordered in a configuration that the neighboring moments are 120° rotated, with the space group $P6_3'cm$.¹⁴ However, the homometric configurations of the Mn^{3+} moments in the triangular lattice are possible to change from each other when lowering temperature or applying magnetic field.^{5–7,10,15,16} The situation would be more complicated for those RMnO_3 with their rare-earth ions having magnetic moments. ErMnO_3 , YbMnO_3 , and HoMnO_3 were found to have a second AF transition at 2.5–4.6 K, below which the long-range AF order of R^{3+} ions are formed.⁷ This low- T AF state can be easily destroyed by a weak magnetic field for

ErMnO_3 and YbMnO_3 , while it is much more stable in magnetic field for HoMnO_3 .⁷ In contrast, TmMnO_3 does not display the long-range order of Tm^{3+} ions although they have pretty large moments.^{7,8,17} Furthermore, the R^{3+} moments were believed to orientate along the c axis with an Ising-like anisotropy but their spin structures are not simple because the R^{3+} ions present in two different crystallographic sites, $2a$ and $4b$.^{7,17–20} Because of the magnetic interaction between the rare-earth ions and the Mn^{3+} ions, the field-induced transitions of Mn^{3+} magnetic structure and the resulted $H - T$ phase diagrams are strongly dependent on the magnetisms of rare-earth ions.^{5–7,10,15,16}

Heat transport has recently been proved to be very useful to probe the spin-phonon coupling and the magnetic transitions in multiferroic materials, including the hexagonal RMnO_3 .^{21–24} In particular, HoMnO_3 was found to have extremely strong magnetic-field dependence of thermal conductivity (κ), which is mainly caused by the magnetic scattering on phonons. An interesting finding was that both the ab -plane and the c -axis magnetic field can induce strong minimum (or “dips”) in $\kappa(H)$ isotherms, which are directly related to the transitions of magnetic structures.²³ In this paper, we study the low- T heat transport of TmMnO_3 , which is a special one in RMnO_3 family because the magnetic ions Tm^{3+} do not form a long-range order.^{7,8,17} It is expected that the magnetic correlation of Tm^{3+} ions might play an important role in the heat transport. To confirm this, the temperature and field dependencies of κ in TmMnO_3 are compared with those in two isostructural variants YMnO_3 and HoMnO_3 . Besides rather strong magnetic-field dependencies of κ , an important result is a sharp dip at 3.5–4 T in $\kappa(H)$ isotherms due to the transition of Mn^{3+} magnetic struc-

ture driven by the c -axis field. In addition, the magnetic field up to 14 T along the ab plane does not induce any magnetic transition. These heat transport behaviors have good correspondence with the magnetization data of TmMnO_3 .

II. EXPERIMENTS

High-quality TmMnO_3 single crystals were grown by using a floating-zone technique in flowing mixture of Ar and O_2 with the ratio 4:1. The crystals were carefully checked by using the x-ray Laue photograph and cut precisely along the crystallographic axes, with parallelepiped shape and typical size of $2.5 \times 0.6 \times 0.15 \text{ mm}^3$ for the heat transport measurements. The thermal conductivities were measured along both the a (κ_a) and the c axes (κ_c) by using a conventional steady-state technique with the temperature down to 0.3 K, which has been described elsewhere.^{23–26} The magnetization was measured using a SQUID-VSM (Quantum Design). The samples for the specific-heat measurements were cut into thin plates with the a or the c axis normal to the basal plane. The specific heat was measured by the relaxation method in the temperature range from 0.4 to 30 K using a commercial physical property measurement system (PPMS, Quantum Design).

III. RESULTS AND DISCUSSION

Before presenting the heat transport data of TmMnO_3 single crystals, we show some characterizations of the magnetization and specific heat. Figure 1 shows the basic magnetic properties of TmMnO_3 single crystals. The magnetic susceptibilities and the inverse susceptibilities along the a and the c axes are essentially the same as those in some earlier literatures.^{7,8} The data show two main results. First, the temperature dependencies of the susceptibilities show some slight changes at ~ 84 K, which indicates the AF transition of Mn^{3+} moments. These changes can be more easily detected from the temperature dependencies of the inverse susceptibilities. Second, the Tm^{3+} moments do not show long-range order at temperatures down to 2 K. However, the low- T susceptibilities show deviations from the paramagnetic behavior, which include a kink of χ_c and a weak increase of χ_a below 10 K (see Fig. 1(b) and the inset to Fig. 1(a)). These suggest that the magnetic correlations among Tm^{3+} moments are not negligible. The low- T magnetization curves of TmMnO_3 , which are not available from the literature, are useful for indicating the field-induced transitions of magnetic structure. As shown in Fig. 1(c), the magnetic field along the ab plane causes a simple paramagnetic effect. Actually, the $M(H)$ curves are nearly linear up to 7 T except for a small curvature at low fields. Although there was no report on whether there is transition of the magnetic

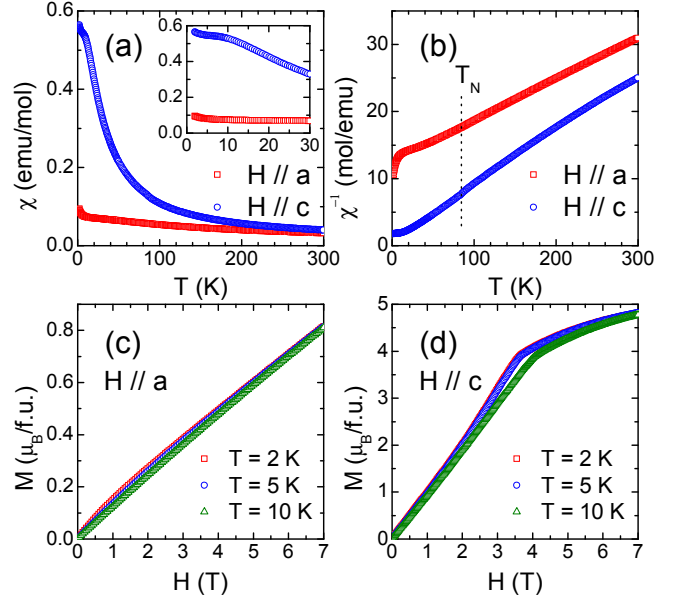


FIG. 1: (color online) (a, b) Temperature dependencies of the magnetic susceptibilities and the inverse susceptibilities of TmMnO_3 for magnetic field (0.1 T) applied along the a and the c axes. Inset to panel (a): low-temperature data of the susceptibilities. The dashed line in panel (b) indicated the slope changes of data at ~ 84 K, which corresponds to the Néel temperature of Mn^{3+} moments. (c, d) Low-temperature magnetization curves of TmMnO_3 for magnetic field along the a and the c axes. The slope changes of $M(H)$ at 3.5–4 T in panel (d) is related to an in-plane spin re-orientation of Mn^{3+} sublattice.

structure for the field along the ab plane, the magnetization curves shown in Fig. 1(c) strongly negate this possibility. In contrast, the $M(H)$ in the c -axis field behaves very differently. First of all, the magnetization is much larger in the c -axis field, which is consistent with the $\chi(T)$ data and indicates that the spin-easy axis of Tm^{3+} ions is along the c direction.^{7,8} In addition, there is a clear transition at 3.5–4 T for temperatures from 2 to 10 K. It is coincided with a field-induced transition of Mn^{3+} magnetic structure from $P6'_3c'm$ to $P6_3c'm'$, proposed from the earlier dielectric measurements.⁷ The feature of $M(H)$ across this transition is the most similar to that in ErMnO_3 among all hexagonal manganites.⁷ It needs to be pointed out that, however, there is by now no clear explanation for the sharp change of the $M(H)$ slope at this transition, although it should be a direct response of the Tm^{3+} moments since the Mn^{3+} moments are known to have no component along the c axis. The earlier Mössbauer spectra indicated that the Tm^{3+} ions on the $4b$ site have AF interactions and those on the $2a$ site are simply paramagnetic.¹⁷ It is likely that the slope changes of magnetization curves for $H \parallel c$ is a spin flip transition of the $4b$ moments, considering their strong spin anisotropy. The slower increase of magnetization above this field is the paramagnetic contribution from the $2a$ moments. In addition, the magnetization for $H \parallel a$ is

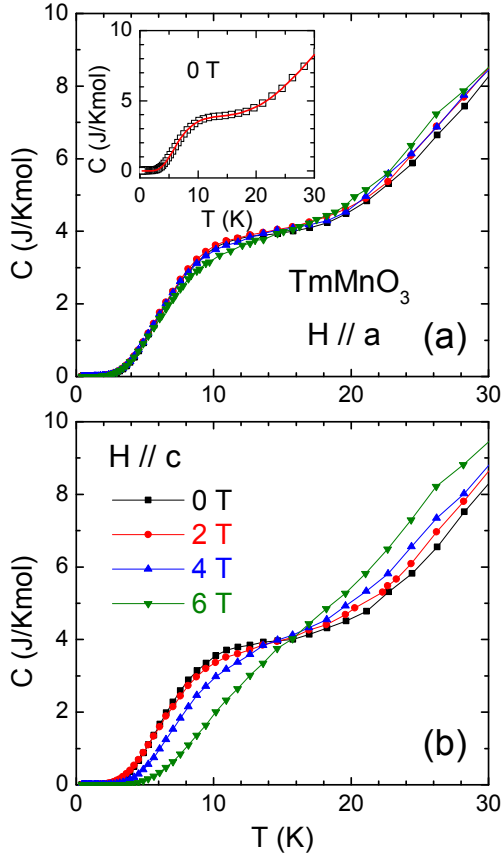


FIG. 2: (color online) Low-temperature specific heat of TmMnO₃ single crystals for magnetic fields along the *a* and the *c* axes, respectively. The hump at ~ 4 –16 K is very robust under the in-plane field but gradually smeared out by the *c*-axis field. Inset to panel (a): the zero-field data and a fitting result, indicated by the solid line, by using formula (1).

mainly the paramagnetic response of the $2a$ moments.

Figure 2 shows the specific-heat data of TmMnO₃ single crystals at low temperatures and in magnetic fields along the *a* and the *c* axes, respectively. The zero-field data indicates no phase transition down to 0.4 K. However, there is a hump-like feature in temperature range from 4 to about 16 K, which makes the temperature dependence not to be described by the standard phonon behavior. Apparently, this feature is caused by some magnetic contributions. The magnetic fields suppress the specific heat below ~ 16 K but enhance the specific heat above ~ 16 K, signifying a Schottky anomaly from the paramagnetic ions. It is useful to try a fitting to the zero-field data by considering both the phononic formula and that of a simple Schottky formula for a two-level system, that is,

$$C(T) = \beta T^3 + \beta_5 T^5 + \beta_7 T^7 + N \left(\frac{\Delta}{k_B T} \right)^2 \frac{e^{\Delta/k_B T}}{(1 + e^{\Delta/k_B T})^2}. \quad (1)$$

The parameters β , β_5 , and β_7 describe the phononic specific heat using the low-frequency expansion of the De-

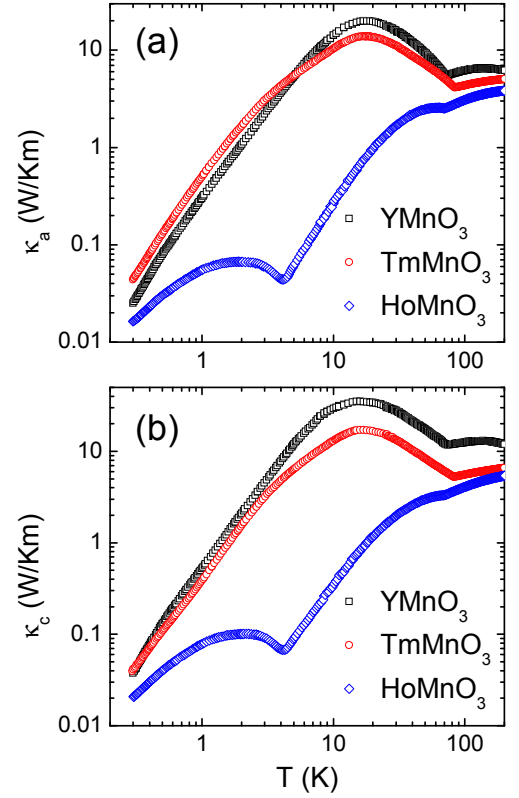


FIG. 3: (color online) Temperature dependencies of the *ab*-plane and the *c*-axis thermal conductivities of TmMnO₃ single crystals. The data of YMnO₃ and HoMnO₃ single crystals taken from Ref. 23 are also shown for comparison.

bye function $C_p = \beta T^3 + \beta_5 T^5 + \beta_7 T^7$.²⁷ Δ is the splitting of the ground-state doublet of magnetic ions and the concentration of free spins is N/R , with R the universal gas constant.^{26,27} The fitting can be pretty good, as shown in the inset to Fig. 2(a) with the parameters $\beta = 2.6 \times 10^{-4}$ J/K⁴mol, $\beta_5 = 1.21 \times 10^{-7}$ J/K⁶mol, and $\beta_7 = -1.31 \times 10^{-10}$ J/K⁸mol, $N = 7.59$ J/Kmol, and $\Delta = 2.36$ meV. The fitting parameters for the phononic specific heat are comparable with those in other RMnO₃ compounds.^{28,29} The value of fitting parameter Δ is also comparable to that from the analysis on Mössbauer spectra.¹⁷ This indicates that the magnetic specific heat is mainly from a Schottky anomaly of Tm³⁺ ions, which do not form a long-range ordered state at low temperatures. However, it is notable that the effect of magnetic field on the magnetic specific heat is much larger with $H \parallel c$ than with $H \parallel a$, showing a phenomenon different from a pure Schottky anomaly. Actually, the field up to 6 T along the *a* axis seems to produce very weak Zeeman splitting of the ground-state doublet. This indicates that the short-range magnetic correlations of Tm³⁺ ions on the $4b$ sites should be involved. In this regard, both the specific heat and magnetic susceptibility show a dominant paramagnetic behavior of Tm³⁺ moments, but with unnegligible magnetic correlations.

Figure 3 shows the temperature dependencies of κ_{ab} and κ_c of TmMnO₃ single crystals in zero field, together with those of YMnO₃ and HoMnO₃ for comparison.²³ The same feature of these three materials is that the thermal conductivities show clear “kinks” at the Néel temperatures of Mn³⁺ moments, which is about 84 K for TmMnO₃. It is known to be due to the strong phonon scattering by the spin fluctuations.^{21–23} The low- T heat transport behaviors of these materials seem to be strongly affected by the magnetic properties of the rare-earth ions. For YMnO₃, in which the Y³⁺ ions are nonmagnetic, the low- T heat transport is a typical one in insulating crystals,³⁰ with large phonon peaks at 15 K indicating the high quality of the crystals. For HoMnO₃, another strong “dip” shows up in the $\kappa(T)$ curves at the Néel temperature of Ho³⁺. Due to the strong spin fluctuations related to the multiple AF ordering and magnetic structure transitions, the phonon heat transport of HoMnO₃ is so strongly suppressed that the κ can be 1–2 orders of magnitude smaller than that of YMnO₃. For TmMnO₃, the Tm³⁺ ions are magnetic but there is no long-range order of their moments. As the susceptibility and specific-heat data suggest, the magnetic correlations or some short-range order are established among the Tm³⁺ moments at low temperatures. As a result, the magnetic fluctuations of Tm³⁺ cannot be neglected. The $\kappa(T)$ data in Fig. 3 show that although the very-low- T thermal conductivities of TmMnO₃ are comparable or even larger than those of YMnO₃, the magnitudes of phonon peaks (also locating at ~ 15 K) are much smaller in TmMnO₃. In addition, the $\kappa(T)$ curves of TmMnO₃ show some slight curvatures at 4–10 K, which indicates a resonant-scattering on phonons, probably by paramagnetic ions.

Before proceeding on studying the effect of magnetic field on the heat transport of TmMnO₃, we show in Fig. 4 some representative low- T $\kappa(H)$ isotherms of YMnO₃ single crystals, of which the $\kappa(T)$ data were already shown in Fig. 3. It is clear that the field dependence of κ is not strong in YMnO₃ and is probably related to some scattering effect by the magnetic impurities or defects.^{33,34} In passing, this magnetic scattering is likely the reason that the very-low- T κ of YMnO₃ show a weaker temperature dependence than T^3 . Furthermore, the field dependencies of κ are generally rather smooth and there is no any drastic change, which means that neither the c -axis nor the ab -plane fields induce any transitions of the ground state and the magnetic structure. This is in good consistency with the earlier works.⁴

The magnetic field is found to strongly affect the heat transport of TmMnO₃. As shown in Fig. 5, the effect of magnetic field on the low- T thermal conductivities depends on the direction of field and are nearly the same for different directions of heat current. In magnetic field along the a axis, both the κ_a and the κ_c show an increase at subKelvin temperatures and a decrease at higher temperatures. It is notable that the slight curvatures of the zero-field $\kappa(T)$ curves at 4–10 K are clearly enlarged in

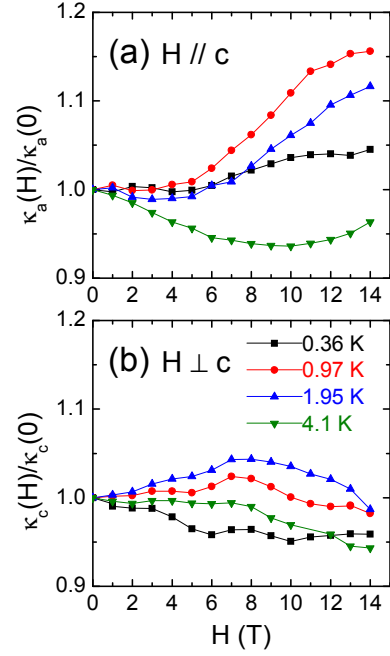


FIG. 4: (color online) Magnetic-field dependencies of κ_a and κ_c of YMnO₃ single crystals at low temperatures. The magnetic field is along and perpendicular to the c axis, respectively.

the 5 T and 14 T curves and a shoulder-like feature is visualized. This confirms the phonon resonant scattering behavior.^{25,30} When applying magnetic field along the c axis, the heat transport changes in a different way. The low fields of 3.5 T and 4 T can suppress the thermal conductivities in the whole temperature range, while a high field of 14 T ($\parallel c$) can significantly enhance the thermal conductivities, particularly at temperatures around 10 K. A common feature for the $\kappa(T)$ in either $H \parallel a$ or $H \parallel c$ is that 14 T field always increases the conductivity at subKelvin temperatures.

From the $\sim T^2$ dependencies of the zero-field conductivities at subKelvin temperatures, which are much weaker than the standard T^3 law of phonon conductivity at the boundary scattering limit, it is easy to know that the microscopic phonon scatterings are still effective at such low temperatures.³⁰ Since the crystal defects scattering on phonons usually fades away with decreasing temperature below 1 K,³⁰ the phonons are mainly scattered by magnetic excitations or spin fluctuations.^{23,24} Therefore, the high-field-induced increase of κ at low temperatures indicates that the magnetic scattering can be removed by high magnetic field.^{23,24} It can be known that the magnetic scattering is mainly related to the Tm³⁺ sublattice. On the one hand, although the Mn³⁺ moments are antiferromagnetically ordered at low temperatures, the strong spin anisotropy of Mn³⁺ ions and the resulted anisotropy gap in the magnon spectrum^{12,31,32} make the low-energy Mn³⁺ magnon excitations impossible at very low temper-

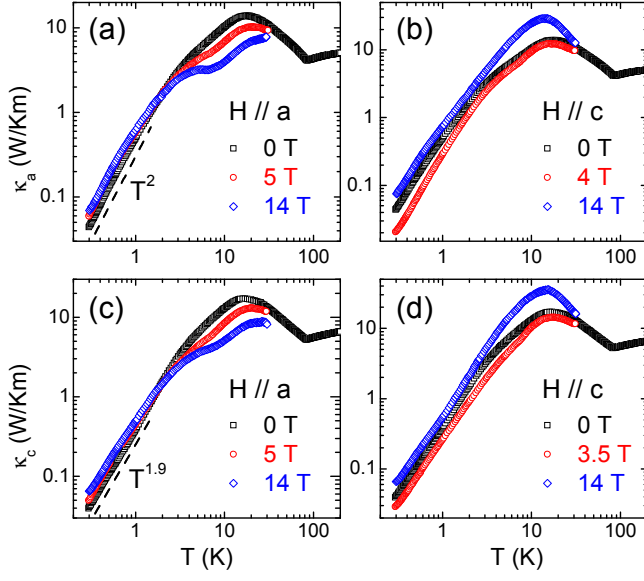


FIG. 5: (color online) Temperature dependencies of thermal conductivities of TmMnO₃ single crystals for κ_a (a-b) and κ_c (c-d) in both the zero field and several different magnetic fields up to 14 T. The dashed lines in panels (a) and (c) indicate the temperature dependencies of the zero-field κ at subKelvin temperatures.

atures. On the other hand, the Tm³⁺ moments do not form a long-range ordered state but are antiferromagnetically correlated. It is also notable that the phonon peaks of $\kappa_a(T)$ and $\kappa_c(T)$ in 14 T field are comparable or even larger than those of YMnO₃. This means that the phonon thermal conductivities of these RMnO₃ are essentially the same if the magnetic scattering effect is negligible.

The detailed magnetic-field dependencies of the low- T thermal conductivities of TmMnO₃ are shown in Fig. 6, which are apparently much stronger than those of YMnO₃ but weaker than those of HoMnO₃.²³ First of all, as the $\kappa(T)$ data already indicated, the field-dependencies of κ are mainly dependent on the direction of magnetic field rather than that of heat current. And there are some important features of these $\kappa(H)$ isotherms that the $\kappa(T)$ data cannot reveal. The most remarkable behavior is the sharp “dips” in $\kappa(H)$ curves for $H \parallel c$ and the positions of these minimums of κ are temperature independent from 0.36 to 7.5 K, which are very similar to the phenomenon observed in HoMnO₃.²³ It has been known that TmMnO₃ has a field-induced spin re-orientation for $H \parallel c$. The transition field is decreased with lowering temperature from ~ 60 K and becomes weakly temperature dependent (about 4.2 T) below 10 K.⁷ Therefore, it is clear that the dips in $\kappa(H)$ curves correspond to this field-induced transition of magnetic structure. One may note that the dip fields are a bit different in $\kappa_a(H)$ and $\kappa_c(H)$ curves, which are at 3.5 and 4 T, respectively. It is understandable if the demagnetization effect is taken into account. The samples for

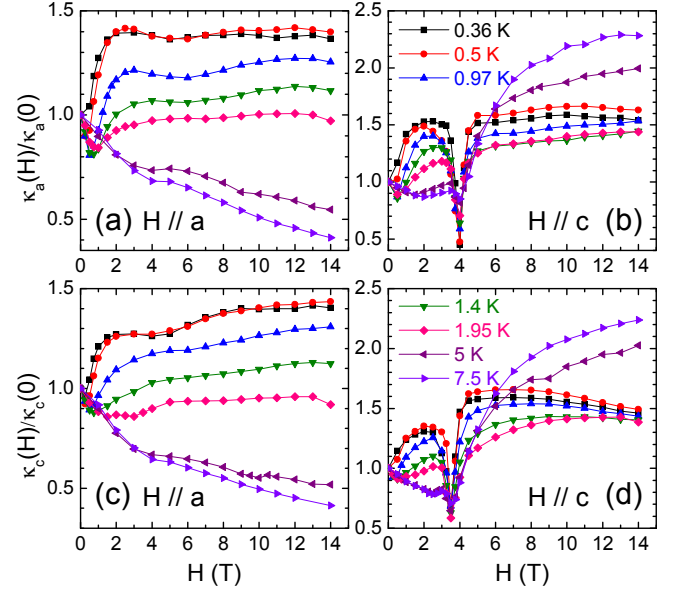


FIG. 6: (color online) Magnetic-field dependencies of κ_a and κ_c of TmMnO₃ single crystals at low temperatures. The magnetic field is along either the a or the c axis.

κ measurement are shaped into long-bar-like, with the longest dimensional along the heat current. Therefore, for κ_a and κ_c samples, the c -axis fields are applied to the dimensions along the thickness and length, respectively, which yields rather different demagnetization factors for these two measurements. According to the sample sizes, the demagnetization factors are calculated to be 0.748 and 0.048 for κ_a and κ_c samples, respectively. Using the susceptibility data from Fig. 1, the difference in the (external) transition fields for these two samples can be calculated and is about 15%,²⁴ which is in good consistent with the experimental observation.

The $\kappa(H)$ behaves rather differently in the case of $H \parallel a$; in particular, there is no similar sharp dip-like feature. It is consistent with the magnetization data of Fig. 1(c) in the regard that there is no transition of magnetic structure for field along the ab plane. The overall field dependencies of κ , apart from the strong dips at 3.5–4 T, are also somewhat different for $H \parallel a$ and $H \parallel c$. At the lowest temperature of 0.36 K, the $\kappa(H)$ isotherms are very similar in different field directions; that is, the κ show a quick increase at low fields and become nearly field independent above 2 T (except for the strong dip for $H \parallel c$). With increasing temperature up to ~ 1 K, the $\kappa(H)$ isotherms in different field directions are still rather similar, including the appearance of a small dip at low fields. Actually the features of a low-field dip and a high-field plateau in $\kappa(H)$ curves are qualitatively the same as that caused by the paramagnetic scattering on phonons.^{26,33,34} A significant difference between $H \parallel a$ and $H \parallel c$ appears at high temperatures. It can be seen that $\kappa(H)$ at 5 and 7.5 K show continuous suppressions for $H \parallel a$ and strong high-field increases for

$H \parallel c$, respectively. It seems that this difference has some correspondence with the field dependencies of specific heat shown in Fig. 2. Therefore, it is possible to understand this result using the paramagnetic scattering scenario,^{26,33,34} in which the magnetic scattering can be strong in the former case but would be removed in the latter case.

At last, it would be useful to compare the heat transport of TmMnO_3 with that of HoMnO_3 . In an earlier work, some dip-like anomalies have also been observed in the low- T $\kappa(H)$ isotherms of HoMnO_3 at the field-induced transitions of magnetic structure.²³ Those results suggested that Ho^{3+} moments form two AF sublattices and undergo two transitions upon increasing field along the c axis, accompanied with two spin re-orientations of the Mn^{3+} sublattice. In addition, the $\kappa(H)$ data for $H \parallel ab$ revealed that a spin re-orientation of Mn^{3+} sublattice could also occur even when the Ho^{3+} sublattice may not be affected. In contrast, the magnetic transitions evidenced by the heat transport as well as the magnetization are simpler in TmMnO_3 . Another difference between TmMnO_3 and HoMnO_3 is that the magnetic-field dependencies of κ are at least several times larger in HoMnO_3 . In fact, HoMnO_3 has very small zero-field κ and the significant increase of conductivity at high magnetic field.²³ Apparently, the mechanism for the magnetothermal conductivity can be shared for these two compounds, while the difference of $\kappa(H)$ is due to the stronger R^{3+} - Mn^{3+} magnetic interactions in HoMnO_3 . In this regard, thermal conductivity results provide a transparent demonstration that the spin-phonon coupling in $R\text{MnO}_3$ is mainly determined by the magnetism of R^{3+} and is the strongest in HoMnO_3 .

Although the mechanism of the field-induced re-orientation of Mn^{3+} moments is still not very clear, the magnetic interaction between rare-earth ions and Mn^{3+} ions is obviously very important. In hexagonal $R\text{MnO}_3$, the exchange coupling between R^{3+} and Mn^{3+} ions is weak because their moments are perpendicular to each other. In such case, the dipolar interaction is more important and larger magnetic moment of Ho^{3+} results in stronger interaction.⁷ Nevertheless, the magnetic interactions can be described by the effective fields acting on R^{3+} and Mn^{3+} moments. For magnetic field along the c axis, there is no doubt that the transitions of R^{3+} sublattices cause the re-orientations of Mn^{3+} moments, because the Mn^{3+} moments are so strongly confined in the ab plane that they cannot be in-plane rotated by the mag-

netic field. It is likely that when the R^{3+} moments are re-aligned in the magnetic field, the effective field from the Mn^{3+} lattice may cause an increase of the R^{3+} energy. The choice of a different configuration of the Mn^{3+} spin lattice would be an effective way to lower the magnetic energy and stabilize the magnetic structure. The case for magnetic field along the ab plane could be more complicated. The re-orientations of the Mn^{3+} moments would be irrelevant to the R^{3+} ions if they have extremely strong Ising anisotropy. However, the different magnetic transitions between TmMnO_3 and HoMnO_3 clearly indicate that the rare-earth ions are playing an important role also for $H \parallel ab$. One possibility is that the R^{3+} moments can be canted or tilted to the ab direction by the magnetic field, which results in a change of the effective field on the Mn^{3+} moments and the instability of their orientation. Further quantitative theoretical investigations on the R^{3+} - Mn^{3+} magnetic interactions are needed.

IV. SUMMARY

The low-temperature heat transport of the hexagonal TmMnO_3 shows strong magnetic-field dependencies, which points to a rather strong spin-phonon coupling in this material. A sharp dip-like feature in $\kappa(H)$ isotherms for $H \parallel c$ is found to be due to the transition of magnetic structure, as the magnetization shows. The absence of the sharp transition of κ for $H \parallel a$ indicates that the in-plane field up to 14 T cannot change the magnetic structure. The comparison of transport properties among TmMnO_3 , YMnO_3 and HoMnO_3 confirms that the magnetisms of rare-earth ions are the key to determine the $H - T$ phase diagram and the strength of spin-phonon coupling.

Acknowledgments

This work was supported by the National Natural Science Foundation of China, the National Basic Research Program of China (Grant Nos. 2009CB929502 and 2011CBA00111), and the Fundamental Research Funds for the Central Universities (Program No. WK2340000035).

* Electronic address: xfsun@ustc.edu.cn

¹ M. Fiebig, Th. Lottermoser, D. Fröhlich, A. V. Goltsev, and R. V. Pisarev, *Nature* **419**, 818 (2002).

² T. Lottermoser, T. Lonkai, U. Amann, D. Hohlwein, J. Ihlinger, and M. Fiebig, *Nature* **430**, 541 (2004).

³ B. B. Van Aken, T. T. Palstra, A. Filippetti, and N. A. Spaldin, *Nature Mater.* **3**, 164 (2004).

⁴ M. Fiebig, T. Lottermoser, and R. V. Pisarev, *J. Appl. Phys.* **93**, 8194 (2002).

⁵ M. Fiebig, C. Degenhardt, and R. V. Pisarev, *Phys. Rev. Lett.* **88**, 027203 (2002).

⁶ F. Yen, C. R. dela Cruz, B. Lorenz, Y. Y. Sun, Y. Q. Wang, M. M. Gospodinov, and C. W. Chu, *Phys. Rev. B* **71**, 180407(R) (2005).

- ⁷ F. Yen, C. dela Cruz, B. Lorenz, E. Galstyan, Y. Y. Sun, M. Gospodinov, and C. W. Chu, *J. Mater. Res.* **22**, 2163 (2007).
- ⁸ V. Skumryev, M. D. Kuz'min, M. Gospodinov, and J. Fontcuberta, *Phys. Rev. B* **79**, 212414 (2009).
- ⁹ O. P. Vajk, M. Kenzelmann, J. W. Lynn, S. B. Kim, and S.-W. Cheong, *Phys. Rev. Lett.* **94**, 087601 (2005).
- ¹⁰ N. Hur, I. K. Jeong, M. F. Hundley, S. B. Kim, and S.-W. Cheong, *Phys. Rev. B* **79**, 134120 (2009).
- ¹¹ B. G. Ueland, J. W. Lynn, M. Laver, Y. J. Choi, and S.-W. Cheong, *Phys. Rev. Lett.* **104**, 147204 (2010).
- ¹² E. C. Standard, T. Stanislavchuk, A. A. Sirenko, N. Lee and S.-W. Cheong, *Phys. Rev. B* **85**, 144422 (2012).
- ¹³ N. Iwata and K. Kohn, *J. Phys. Soc. Jpn.* **67**, 3318 (1998).
- ¹⁴ W. C. Koehler, H. L. Yakel, E. O. Wollan, and J. W. Cable, *Phys. Lett.* **9**, 93 (1964).
- ¹⁵ B. Lorenz, F. Yen, M. M. Gospodinov, and C. W. Chu, *Phys. Rev. B* **71**, 014438 (2005).
- ¹⁶ P. J. Brown and T. Chatterji, *Phys. Rev. B* **77**, 104407 (2008).
- ¹⁷ H. A. Salama and G. A. Stewart, *J. Phys.: Condens. Matt.* **21**, 386001 (2009).
- ¹⁸ Th. Lonkai, D. Hohlwein, J. Ihringer, and W. Prandl, *Appl. Phys. A* **74**, S843 (2002).
- ¹⁹ S. Nandi, A. Kreyssig, L. Tan, J.W. Kim, J. Q. Yan, J. C. Lang, D. Haskel, R. J. McQueeney, and A. I. Goldman, *Phys. Rev. Lett.* **100**, 217201 (2008).
- ²⁰ X. Fabrèges, I. Mirebeau, P. Bonville, S. Petit, G. Lebras-Jasmin, A. Forget, G. André, and S. Pailhès, *Phys. Rev. B* **78**, 214422 (2008).
- ²¹ P. A. Sharma, J. S. Ahn, N. Hur, S. Park, S. B. Kim, S. Lee, J.-G. Park, S. Guha, and S.-W. Cheong, *Phys. Rev. Lett.* **93**, 177202 (2004).
- ²² J.-S. Zhou, J. B. Goodenough, J. M. Gallardo-Amores, E. Morán, M. A. Alario-Franco, and R. Caudillo, *Phys. Rev. B* **74**, 014422 (2006).
- ²³ X. M. Wang, C. Fan, Z. Y. Zhao, W. Tao, X. G. Liu, W. P. Ke, X. Zhao, and X. F. Sun, *Phys. Rev. B* **82**, 094405 (2010).
- ²⁴ Z. Y. Zhao, X. M. Wang, C. Fan, W. Tao, X. G. Liu, W. P. Ke, F. B. Zhang, X. Zhao, and X. F. Sun, *Phys. Rev. B* **83**, 014414 (2011).
- ²⁵ X. F. Sun, W. Tao, X. M. Wang, and C. Fan, *Phys. Rev. Lett.* **102**, 167202 (2009).
- ²⁶ Q. J. Li, Z. Y. Zhao, H. D. Zhou, W. P. Ke, X. M. Wang, C. Fan, X. G. Liu, L. M. Chen, X. Zhao, and X. F. Sun, *Phys. Rev. B* **85**, 174438 (2012).
- ²⁷ A. Tari, *Specific Heat of Matter at Low Temperatures* (Imperial College Press, 2003).
- ²⁸ M. Tachibana, J. Yamazaki, H. Kawaji, and T. Atake, *Phys. Rev. B* **72**, 064434 (2005).
- ²⁹ P. Liu, X.-L. Wang, Z.-X. Cheng, Y. Du, and H. Kimura, *Phys. Rev. B* **83**, 144404 (2011).
- ³⁰ R. Berman, *Thermal Conduction in Solids* (Oxford University Press, Oxford, 1976).
- ³¹ S. Petit, F. Moussa, M. Hennion, S. Pailhès, L. Pinsard-Gaudart, and A. Ivanov, *Phys. Rev. Lett.* **99**, 266604 (2007).
- ³² X. Fabrèges, S. Petit, I. Mirebeau, S. Pailhès, L. Pinsard, A. Forget, M. T. Fernandez-Diaz, and F. Porcher, *Phys. Rev. Lett.* **103**, 067204 (2009).
- ³³ X. F. Sun, I. Tsukada, T. Suzuki, S. Komiya, and Y. Ando, *Phys. Rev. B* **72**, 104501 (2005).
- ³⁴ X. F. Sun, A. A. Taskin, X. Zhao, A. N. Lavrov, and Y. Ando, *Phys. Rev. B* **77**, 054436 (2008).